Microscopic Approach to the Structure of Liquid $Al_{80}Mn_{20}$ and $Al_{80}Ni_{20}$ Alloys

L. Do Phuong, D. Nguyen Manh,* and A. Pasturel

Laboratoire de Thermodynamique et Physico-Chimie Métallurgiques, ENSEEG BP75, 38402 Saint Martin d'Hères, France

(Received 8 February 1993)

A new tight-binding-bond approach to interatomic forces in liquid aluminum–transition metal (Al-*M*) alloys is presented. It is shown that the bond order depends strongly on the strength of the *pd* hybridization in the Al-*M* alloy, leading to nonadditive potentials with a strong preference for the formation of a pair of unlike atoms and short bond distances in the Al-*M* pairs. This is illustrated by studying the structural properties of liquid $Al_{80}Ni_{20}$ and $Al_{80}Mn_{20}$ alloys using molecular dynamics simulations and by comparing our results with the available experimental ones.

PACS numbers: 61.20.Ja, 61.25.Mv, 71.25.Lf

Since the discovery of quasicrystalline phases in AlMn alloys [1], icosahedral order in liquid alloys has generated a renewal of interest. Frank [2] was the first to suggest that the structure of liquid metals could be based on icosahedral packing, in order to explain supercooling effects. Thirty years later, this description has been confirmed by molecular dynamics simulation of supercooled liquids [3]. Very recently, Maret and co-workers [4,5] have focused attention on the study of topological and chemical short-range order in liquid $Al_{80}Mn_{20}$ and $Al_{80}Ni_{20}$ alloys, through the accurate determination of the partial pair correlation functions by neutron diffraction. The interest of such a study is that the binary Al_xMn_{1-x} liquids in the region near 20 at.% Mn form icosahedral phases after fast quenching while no such phases have been prepared from Al_xNi_{1-x} liquids. The main conclusion of these experimental studies is that the topological ordering differs significantly in the two alloys, the ordering extending to large distances in $Al_{80}Mn_{20}$ and of short-range order in $Al_{80}Ni_{20}$. It is tempting to correlate the higher degree of topological ordering in the liquid $Al_{80}Mn_{20}$ to the formation of quasicrystalline phases in this system. From the theoretical point of view, the determination of bond-angle distribution by means of molecular dynamics calculations, based on a good representation of the three partial pair distribution functions to the limits of their accuracy, should allow us to differentiate and characterize the local structural motifs in the liquid $Al_{80}Mn_{20}$ and $Al_{80}Ni_{20}$ alloys. However, an accurate simulation of the properties of transition metals and of their alloys is still a challenging problem since bonding is not well described by currently available pair and embedded-atom potentials. In this paper, we present a new approach to interatomic forces in transition metal alloys and apply it to liquid $Al_{80}Mn_{20}$ and $Al_{80}Ni_{20}$ alloys for the first time. This approach is based on the bond-order concept [6,7], in which the actual atomic environment is replaced by a Bethe lattice. This allows for an explicit expression of the bond order as a function of the interatomic distance and leads to an expression for the interatomic forces in terms of strongly nonadditive pair forces. Within the framework of the tight-binding Hückel theory, the quantum-mechanical bond energy in a given pair of atoms i and j is written in the chemically intuitive form:

$$U_{\text{bond}}(i,j)=\sum_{\alpha,\beta}\Phi^{\text{bond}}_{\alpha(i),\beta(j)}=2\sum_{\alpha,\beta}H_{i\alpha,j\beta}\Theta_{j\beta,i\alpha}\,, \tag{1}$$

where $H_{i\alpha,j\beta}$ is the Slater-Koster bond-integral matrix linking the orbitals α,β on sites i and j together. Θ is the corresponding bond-order matrix whose elements give the difference between the number of electrons in the bonding $1/\sqrt{2}|i\alpha+j\beta\rangle$ and antibonding $1/\sqrt{2}|i\alpha-j\beta\rangle$ states. Bond-order potentials are similar to the embedding potentials in that the bond in a given pair of atoms is considered as embedded in and depending on the local atomic environment. Thus Eq. (1) represents only formally a pair interaction and depends via the bond order on many-atom effects. This bond order can be expressed in terms of the integral over the imaginary part of the off-diagonal Green's function,

$$\Theta_{i\alpha,j\beta}=-\frac{2}{\pi}\,\mathrm{Im}\int^{E_F}G_{i\alpha,j\beta}(E)\,dE\,. \tag{2}$$

To calculate such a quantity, we have used the cluster Bethe lattice reference system (CBLM) [8]. Then, it is clear that the many-body expansion in the bond order depends on the size of the cluster embedded in the Bethe lattice. If the cluster is chosen to be the lattice site, a very rapid convergence of the many-body expansion is obtained. Moreover, as this approximation is exact up to the fourth moment, it gives bond potentials which are based on a better many-body expansion than the classical used ones. As in this paper we are dealing with liquid alloys, we present the derivation of the bond potentials within the lattice site approximation.

In this case, the bond order can be written as

$$\Theta_{I\alpha,J\beta}=-\frac{1}{\pi}n_\alpha n_\beta\,\mathrm{Im}\int^{E_F}[h_{\alpha(I),\beta(J)}G_{\alpha(I)}(E)G'_{\beta(J)}(E)]\,dE\,, \tag{3}$$

where n_α,n_β are the degeneracy of orbital subspaces α,β, respectively, and $h_{\alpha(I)\beta(J)}$ are the hopping energies between a state of subspace α of atom I and a state of sub-

0031-9007/93/71(3)/372(4)$06.00

space β of atom J. $G_{\alpha(I)}$ is the Green's function of atom I in the subspace α as given by the CBLM formalism,

$$G_{\alpha(I)}(z)=\left[z-E_{\alpha(I)}-Z\sum_{\beta(J)}p_{IJ}n_{\beta}T^{2}_{\alpha(I),\beta(J)}G'_{\beta(J)}(z)\right]^{-1}, \tag{4}$$

where Z is the coordination number and p_{ij} the pair probability. $T^{2}_{\alpha(I),\beta(J)}$ is the mean square of the matrix element between a state of subspace α of atom i and a state of subspace β of atom j [9] and the Green's function $G'_{\beta(J)}$ can be defined by

$$G'_{\beta(J)}(z)=\left[z-E_{\alpha(I)}-(Z-1)\times\sum_{\gamma(K)}p_{JK}n_{\gamma}T^{2}_{\beta(J)\gamma(K)}G_{\gamma(K)}(z)\right]^{-1}. \tag{5}$$

The advantage of Eq. (3) is that it allows us to estimate the different orbital contributions in the bond energy, in particular to treat the effect of hybridization explicitly. Assuming that the distance dependence of the bond order is negligible against that of the transfer integral [6], we obtain

$$\Phi^{\mathrm{bond}}_{\alpha(I),\beta(J)}=2h_{\alpha\beta}(r_{ij})\Theta_{I\alpha,J\beta}, \tag{6}$$

with the distance dependence of the hopping integral. Here the average integrals are evaluated according to Harrison's power law [10] [$h_{\alpha\beta}(r_{ij})=h_{\alpha\beta}(1)/r^{n}_{ij}$, $n=2$ for s and p orbitals, $n=5$ for d orbitals]. An especially attractive feature of this bond energy representation is that the electronic forces on the atoms are simply obtained by taking derivations of the tight-binding hopping matrix elements. However, the strength of the interaction is proportional to Θ, which is influenced not only by the local environment around atom i, but by more distant atoms. Although this model is relatively simple, it includes in a natural way the nonlocal many-body effects.

The repulsive part of the binding energy is assumed to be given by a sum over pair potentials [11],

$$U_{\mathrm{rep}}=\frac{1}{2N}\sum_{i,j\neq i}\Phi^{\mathrm{rep}}_{ij}(r_{ij}) \tag{7}$$

with

$$\Phi^{\mathrm{rep}}_{ij}(r_{ij})=\sum_{\alpha,\beta}\Phi^{\mathrm{rep}}_{\alpha(I)\beta(J)}(r_{ij})=\frac{1}{2}\sum_{\alpha,\beta}\left[\frac{C_{\alpha(I)}C_{\beta(J)}}{r_{ij}^{m_{\alpha}+m_{\beta}}}\right]^{1/2}. \tag{8}$$

For s-s and p-p interactions, the repulsive pair interaction may be modeled as $\Phi^{\mathrm{rep}}_{\alpha,\alpha}(r_{ij})=C_{\alpha,\alpha}/r^{4}_{ij}$, while for d-d interactions, a stronger power-law dependence $C_{d,d}/r^{10}_{ij}$ is chosen [10]. $C_{\alpha,\alpha}$ ($\alpha=s$, p, or d orbitals) are the only parameters of the model; they are determined from the knowledge of the experimental atomic volume and bulk modulus of the pure metals. To treat the alloying effect, i.e., the AB interactions, we have to determine the attractive and the repulsive parts of the heteroatomic bond potential. The parametrization of the repulsive pair interaction is still done using Eq. (8) with the same $C_{\alpha(A)}$ and $C_{\beta(B)}$ values. To obtain the $h_{A\alpha,B\beta}$ hopping integrals [that is $(ss\sigma)_{AB}$, $(sp\sigma)_{AB}$, $(sd\sigma)_{AB}$, $(pd\sigma)_{AB}$, and $(pd\pi)_{AB}$], we use the geometrical average of hopping integrals given in Table I, which is reasonable in the case of studied alloys. Consequently, no parameters are introduced to describe the alloy properties. At the end, the usual dependence for both hopping integrals and repulsive terms has been modified using the rescaling method proposed by Goodwin, Skinner, and Pettifor [12]. This method is known for generating improved tight-binding parameters which are both transferable and suitable for extensive molecular dynamics simulations. The two scaling parameters of the scaling smoothed step function, i.e., r_c and n_c, have been chosen in such a way that the step is positioned between the first and the second nearest neighbors in the fcc lattice and that the interactions become zero at $L/2$, where L is the linear dimension of the molecular dynamics cell.

The experimental study of topological and chemical short-range order in $Al_{80}Mn_{20}$ and $Al_{80}Ni_{20}$ liquid alloys [4,5] shows that the first distances in both Al-Al and M-M distributions (M = Mn or Ni) differ significantly in the two alloys, pointing out distinct topological ordering, the ordering extending to large distances in $Al_{80}Mn_{20}$ and being short range in $Al_{80}Ni_{20}$. This feature is emphasized in reciprocal space by the height difference observed for the first peak of the number-number structure factor $S_{NN}(q)$ in the Bhatia-Thornton formalism. Then it is important to know if our interactions are able to reproduce such differences. Therefore the molecular dynamic simulations of liquid $Al_{80}Mn_{20}$ and $Al_{80}Ni_{20}$ alloys were performed at constant volume and constant temperature. We consider a system of 691 Al atoms and 173 M atoms in a cubic box with periodic boundary conditions such that the densities of the two systems are equal to the experimental ones. The initial atomic positions are randomly chosen. The Newtonian equations of motion were solved using the Verlet algorithm with a time increment of 3×10^{-15} s. Typical runs took 40000–50000 steps for melting and equilibration and about as many for production. The Bhatia-Thornton partial structure factors

TABLE I. Tight-binding and repulsive parameters for Al, Mn, and Ni (in eV).

	$ss\sigma$	$dd\sigma$	$dd\pi$	$dd\delta$	$sd\sigma$	$pp\sigma$	$pp\pi$	$sp\sigma$	Css	Cdd	Cpp
Al	−0.52					1.20	−0.31	0.71	0.30		0.30
Mn	−1.33	−0.65	0.32	0.00	−1.15				1.64	0.14	
Ni	−1.42	−0.56	0.28	0.00	−1.11				0.50	0.28	

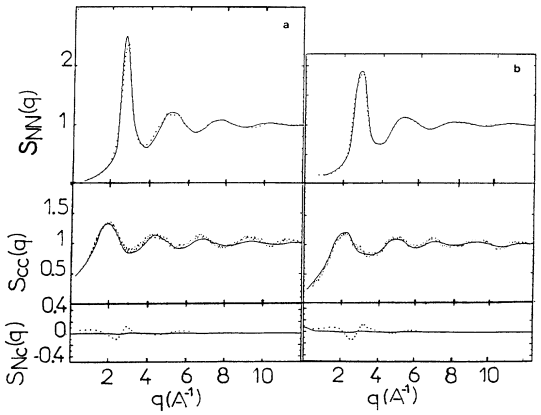

FIG. 1. Comparison between theoretical and experimental Bhatia-Thornton partial structures: (a) liquid $Al_{80}Mn_{20}$ (——) simulation, (····) Ref. [4]; (b) liquid $Al_{80}Ni_{20}$ (——) simulation, (····) Ref. [5].

(PSF) shown in Fig. 1 are based on averages of over 50 independent configurations taken at intervals of 100 time steps. They are perfectly in phase with the experimental curves and, more particularly, reproduce the experimental height of the first and second peaks of $S_{NN}(q)$ for both $Al_{80}Mn_{20}$ and $Al_{80}Ni_{20}$ liquids. The theoretical results presented here allow us to point out clues that indicate icosahedral order in the $S_{NN}(q)$ function of liquid $Al_{80}Mn_{20}$, which are absent for liquid $Al_{80}Ni_{20}$. These arguments are the following ones: (i) There is a large difference between both liquids in the height and the shape of the first peak [$S_{NN}(q_1)=2.45$ with $q_1=2.85$ Å^{-1} for $Al_{80}Mn_{20}$ and $S_{NN}(q_1)=1.92$ with $q_1=2.95$ Å^{-1} for $Al_{80}Ni_{20}$]. Since the ratio of atomic volumes of both species is similar in both systems [see functions $S_{Nc}(q)$], such a change in $S_{NN}(q)$ is attributed to a variation of the spatial extent ξ of topological ordering. ξ can be estimated from the breadth of the first peak of $S_{NN}(q)$ using the Scherrer particle broadening equation $2\pi/\Delta q_{NN}$ [5]. The values of ξ found for $Al_{80}Ni_{20}$ and $Al_{80}Mn_{20}$ are 7 and 10 Å, respectively; this means that atoms in $Al_{80}Mn_{20}$ are arranged roughly over one more interatomic distance than in $Al_{80}Ni_{20}$. (ii) The change in the second peak of $S_{NN}(q)$ is also quite visible; in particular, the second peak for $Al_{80}Ni_{20}$ is rounded while the one for $Al_{80}Mn_{20}$ has a flat top, which from Ref. [13] could be suggestive of short-range icosahedral order.

The first and second oscillations of the two functions $S_{cc}(q)$ are comparable in amplitude but those for $Al_{80}Ni_{20}$ are shifted towards higher q. The spatial extent of chemical ordering deduced from the breadth of the first peak is about twice as small as the one of topological ordering. All these results are confirmed by an analysis of the atomic arrangements between aluminum and transition metal atoms in the first shell. The experimental distribution of the first distances Ni-Ni is split into two components at 2.36 and 2.98 Å. It is quite different from

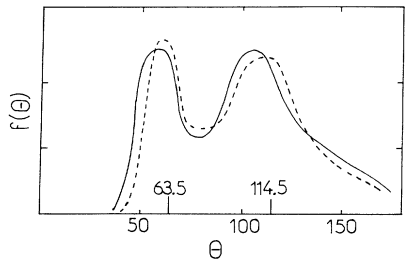

FIG. 2. Calculated bond-angle distributions: (——) liquid $Al_{80}Mn_{20}$, (---) liquid $Al_{80}Ni_{20}$.

the distribution of the first distances Mn-Mn centered at 2.89 Å. Our results fail to reproduce the double-peak structure of contacts Ni-Ni in $Al_{80}Ni_{20}$ but give the general trend that the average first and second M-M distances are shorter in $Al_{80}Ni_{20}$. Indeed, we find r_{MM} equal to 2.55 Å in $Al_{80}Ni_{20}$ while it is equal to 2.86 Å in $Al_{80}Mn_{20}$. This difference cannot be attributed to the very small atomic size difference between Ni and Mn atoms (note that the nearest distances are 2.53 and 2.67 Å in Ni and Mn pure liquids [14]), and suggests different local structural arrangements. This is also supported by the first Al-Al distances significantly shorter than Mn-Mn contacts in $Al_{80}Mn_{20}$ and greater than Ni-Ni contacts in $Al_{80}Ni_{20}$. Experimental data give $r_{AlAl}=2.82$ and 2.74 Å for $Al_{80}Ni_{20}$ and $Al_{80}Mn_{20}$, respectively, while theoretical analysis gives 2.78 and 2.76 Å. The distributions of the first heteroatomic pairs are centered at the same position (2.54 Å for experiments and 2.55 Å for calculations), which corresponds to short distances in comparison with M-M and Al-Al contacts.

The fact that the topological short-range order is different in both alloys is also confirmed by the bond-

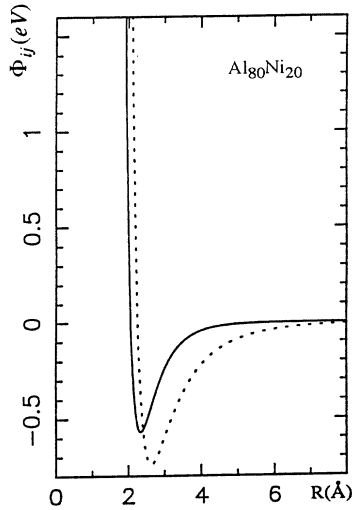

FIG. 3. Ni-Al tight-binding-bond potentials (eV): (····) total, (——) *pd* contribution.

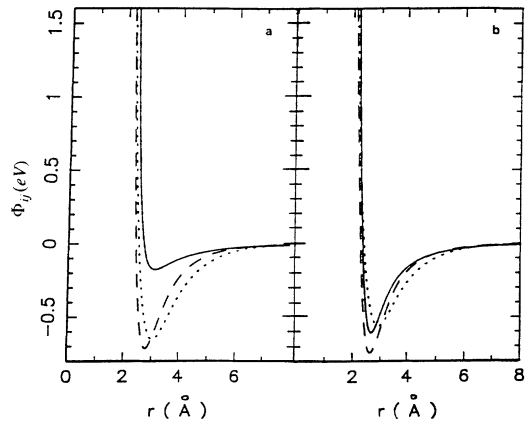

FIG. 4. Tight-binding-bond potentials (eV): (——) *M-M* interaction, (---) *M*-Al interaction, (····) Al-Al interaction. (a) $Al_{80}Mn_{20}$; (b) $Al_{80}Ni_{20}$.

angle distribution functions (see Fig. 2). For $Al_{80}Mn_{20}$, the calculated distribution shows a prominent peak near 63° and a broad maximum near 115°, very close to the icosahedral bond angles of $\theta=63.5°$ and $\theta=116.5°$. For $Al_{80}Ni_{20}$, the distribution is shifted towards smaller bond-angle values and the peak near 60° is less prominent than in $Al_{80}Mn_{20}$. These changes may now be traced back to the variation of the interatomic forces and of the electronic structure. For liquid $Al_{80}Ni_{20}$ alloy, Fig. 3 compares the total Al-*M* tight-binding-bond potential with the partial one obtained by using the *pd* contribution only. We can see that the *pd* hybridization is very strong and represents the major part of the heteroatomic bond potential, leading to a strong interaction between Al and *M* atoms for both liquids. The same behavior is obtained for liquid $Al_{80}Mn_{20}$ alloy. As shown in Fig. 4, that is reflected in a strong nonadditivity of the bond potentials and the consequence is the formation of a pair of unlike atoms and short bond distances in the Al-*M* pairs. But an important difference is between Ni-Ni and Mn-Mn interactions. The Mn-Mn interaction is found to be very small in comparison with Ni-Ni interactions and also Al-Al or Al-*M* interactions. It can be thought that it is the peculiar behavior of Mn-Mn interactions which can explain the difference of topological ordering in $Al_{80}Mn_{20}$ and $Al_{80}Ni_{20}$.

In conclusion, we have developed a new interatomic force field for liquid transition-metal–aluminum alloys which we believe contains an important improvement: the dependence of the pair interaction on the bond order determined by the strength of the *pd* hybridization. We have shown that applications to simulations of $Al_{80}Mn_{20}$ and $Al_{80}Ni_{20}$ liquid alloys are very promising. This will allow the study of the structure-property relationship of these materials at a level of detail not previously possible.

D.N.M. wishes to acknowledge CNRS for financial support. A.P. thanks J. Hafner for helpful discussions. Laboratoire de Thermodynamique et Physico-Chimie Metallurgiques is CNRS UA 29.

*Permanent address: Department of Physics, Polytechnic University of Hanoi, Viet Nam.

[1] D. Shechtman, I. Blech, D. Gratias, and J. W. Cahn, Phys. Rev. Lett. **53**, 1951 (1984).
[2] F. C. Frank, Proc. R. Soc. London A **215**, 43 (1952).
[3] P. J. Steinhardt, D. R. Nelson, and M. Ronchetti, Phys. Rev. B **28**, 784 (1983).
[4] M. Maret, A. Pasturel, C. Senillou, J. M. Dubois, and P. Chieux, J. Phys. (Paris) **50**, 295 (1989).
[5] M. Maret, T. Pomme, A. Pasturel, and P. Chieux, Phys. Rev. B **42**, 1598 (1990).
[6] D. G. Pettifor, Phys. Rev. Lett. **63**, 2480 (1989).
[7] D. G. Pettifor, in *Many-Atom Interactions in Solids*, edited by R. M. Nieminen, M. J. Puska, and M. J. Manninen (Springer-Verlag, Berlin, 1990), p. 64.
[8] L. Do Phuong, D. Nguyen Manh, and A. Pasturel, J. Phys. Condens. Matter **5**, 1901 (1993).
[9] D. Mayou, D. Nguyen Manh, A. Pasturel, and F. Cyrot-Lackmann, Phys. Rev. B **33**, 3384 (1986).
[10] W. A. Harrison, *Electronic Structure and the Properties of Solids* (Freeman, San Francisco, 1980).
[11] A. P. Sutton, M. W. Finnis, D. G. Pettifor, and Y. Ohta, J. Phys. C **21**, 35 (1988).
[12] L. Goodwin, A. J. Skinner, and D. G. Pettifor, Europhys. Lett. **9**, 701 (1989).
[13] S. Sachdev and D. R. Nelson, Phys. Rev. B **32**, 4592 (1985).
[14] Y. Waseda, in *Liquid Metals—1976*, edited by R. Evans and D. A. Greenwood, IOP Conf. Proc. No. 30 (Institute of Physics and Physical Society, Bristol, 1977), p. 230.